ISSN : 0974 - 7486 Volume 12 Issue 4

Materials Science

An Indian Journal

Full Paper

MSAIJ, 12(4), 2015 [125-133]

Thermodynamic calculations describing the solidification of a {m,m'}-based {30Cr, 1C, 15Ta} containing alloy and microstructure comparison with the alloy really elaborated. Part 2:{m,m'}={Co,Fe}

Gaël Pierson[1,2], Kevin Duretz[1,2], Patrice Berthod[1,2,3]*

[1]University of Lorraine, (FRANCE)

[2]Faculty of Sciences and Technologies, (FRANCE)

[3]Institut Jean Lamour (UMR 7198), Team 206 "Surface and Interface, Chemical Reactivity of Materials", (FRANCE)

B.P. 70239, 54506 Vandoeuvre-lès-Nancy, (FRANCE)

E-mail : Patrice.Berthod@univ-lorraine.fr

ABSTRACT

In this second part of the work, an alloy based on Cobalt and Iron with similar contents, containing 30 wt.% Cr again as well as 1 wt.%C and 1 wt.%Ta for obtaining many TaC carbides, was the subject of preliminary thermodynamic calculations to get a description of its microstructure development from the molten state to the solid state at 500°C. A real alloy was thereafter produced by casting from pure elements to allow characterizing the microstructure really obtained. Thermodynamic calculations predicted that solidification should start here too by TaC carbides, before the matrix development itself. This was effectively verified in the real alloy with the presence of blocky TaC carbides which are of a pro-eutectic nature. However some disagreements appeared concerning the chromium carbides notably, which were seen much more present in the real alloy than predicted by thermodynamic calculations. The limitation of the outwards migration of the pro-eutectic carbides was less understood than in the first part, since no so obvious relation between the solidification temperature range and the amount of blocky carbides in the ingot core was revealed. The Vickers hardness of the real alloy is of about 430 Hv_{30kg}.

KEYWORDS

Cobalt;
Iron;
Tantalum carbides;
Thermodynamic calculations;
Solidification;
Microstructures;
Hardness.

INTRODUCTION

Cobalt and iron are rarely present in equivalent proportions in alloys. When it exists in cobalt-based superalloys for example, the content in iron is generally rather low. At the same time cobalt is not an usual element in steels. Cobalt-based alloys as well as iron-based alloys are much common than alloys simultaneously based on cobalt and iron.

Indeed, chromium-rich cobalt-based alloys can be encountered in many applications, from cryogenic/ambient/body temperatures, as prosthetic dentistry[1], up to very high temperatures (e.g. aero-engines[2], industrial processes[3]), where corrosion resistance in corro-

sive aqueous milieus or resistance against high temperature oxidation by gases or hot corrosion by molten salts or CMAS glasses are required[4]. Many of them also contain carbon which allows the development of carbides useful for high mechanical resistance at high temperature (e.g. for combating creep deformation)[5]. Some versions especially rich in carbon and highly alloyed with carbides-former elements can be used to take benefit from the intrinsic rather high hardness of cobalt and the high hardness of carbides, for example as cutting tools[6] made of a cobalt matrix hardened with high amounts of dispersed tungsten carbides, or for Co-W_2C coatings[7] for improving wear resistance of some metallic alloys.

The alloys based on iron are also numerous. Many of them contain carbon too and they often present a rather high hardness, which can vary over a rather wide range because of the presence of hard phases or compounds obtained by fast solidification[8] or by quenching in solid state from the austenitic temperature range[9]. These ones can be the iron carbide Fe_3C cementite, the eutectoid compound {ferrite + cementite} named pearlite, or the unstable phase martensite. Such hard particles or compounds can be found first in simple binary Fe-C alloys but also in more complex iron-based alloys, for instance those containing also chromium (which belongs to the carbide-forming and carbide-stabilizer elements) especially added to enhance the hardness of bulk iron-based materials[10] as well as coatings[11]. The presence of such phases or compounds induce great values of hardness, results which can be wished (for favouring wear resistance for example) or not (for preserving ductility). The same phases also favouring brittleness it is often necessary to control if such phases are present or not in the microstructure, what can be simply done by hardness measurement[12].

Alloys based on simultaneously cobalt and iron appear additionally much rarer when one looks for the presence of tantalum carbides, notably in high quantities. Thus, in order to explore the microstructure of such alloys we first carried out preliminary thermodynamic calculations, and second elaborated and characterized a real alloy. The subject of this second article is to present the results of this work.

EXPERIMENTAL

The chemical composition of interest is basically {27Co-27Fe-30Cr-1C-15Ta}, all contents being in weight percentage. Such composition ought to lead to a {Co,Fe}-based alloy possibly with high TaC fractions and simultaneously resistant against high temperature corrosion.

This work started with preliminarily thermodynamic calculations, in order to get previsions about the development of the microstructure during solidification and solid state cooling. This was realized by using the Thermo-Calc version N software[13], with a database developed from the SSOL database[14] enriched to contain the descriptions of many of the sub-systems of the quinary {Co, Fe, Cr, C, Ta} one[15-26]. Calculations were used to predict the appearance and disappearance of the successive phases, their theoretic mass fractions and chemical compositions versus temperature, from the start of solidification down to 500°C, temperature at which it can be reasonably considered that additional solid state transformations have not time to occur, at least with atomic diffusion.

In parallel this alloy was also elaborated by foundry under 300mbars of pure Argon from pure elements (Co, Fe, Cr and Ta: Alfa Aesar, purity higher than 99.9 wt.%; and C: graphite) placed in the water-cooled copper crucible of a CELES high frequency induction furnace. The latter one was used for achieving melting, with as operating parameters: atmosphere of 300 mbars of pure Ar, voltage up to 4kV, alternative current frequency about 100kHz, (almost) isothermal stay at high temperature in the liquid state: 3 minutes. The solidification of the obtained liquid alloy was achieved by progressively lowering power. The alloy solidified in the water–cooled copper crucible of the HF furnace.

The obtained ingot, of about forty grams, was cut in two half parts. One of them was used to characterize the microstructure of the as-cast alloy over the whole ingot, in order to reveal possible heterogeneities and to take this into account for future tests or investigations. The half part under consideration was embedded in a cold resin mixture (resin CY230 + hardener HY956 from ESCIL – Lyon, France), then ground first with SiC papers from 240 to 1200 grit. Thereafter, after intermùediate ultrasonic cleaning, final polishing was performed using a textile disk enriched with 1µm alumina particles. The metallographic characterization was done using a Scanning Electron Microscopy (SEM JEOL JSM-6010LA) under an acceleration voltage of

20kV, in the Back Scattered Electrons mode (BSE) for the microstructure observations, and with the Energy Dispersion Spectrometry (EDS) apparatus for the global and pinpoint chemical composition measurements. The surface fractions of the carbides were determined by using the basic image analysis tool of the Photoshop CS software (Adobe). Hardness indentation was performed in six locations, using a Testwell Wolpert apparatus (technique: Vickers, load: 30kg).

RESULTS AND DISCUSSION

The main solidification and solid state transformation steps according to Thermo-Calc

Many thermodynamic calculations were performed with Thermo-Calc to better know the genesis of the microstructure. The obtained description supposes that the thermodynamic equilibrium is respected at each step, which is generally not the case for solidification and cooling of real alloys. Results (number, natures and mass fractions) are graphically given in Figure 1.

The value of liquidus temperature automatically determined by Thermo-Calc is 1693.94°C. The first crystals to appear are not metallic but carbides. These

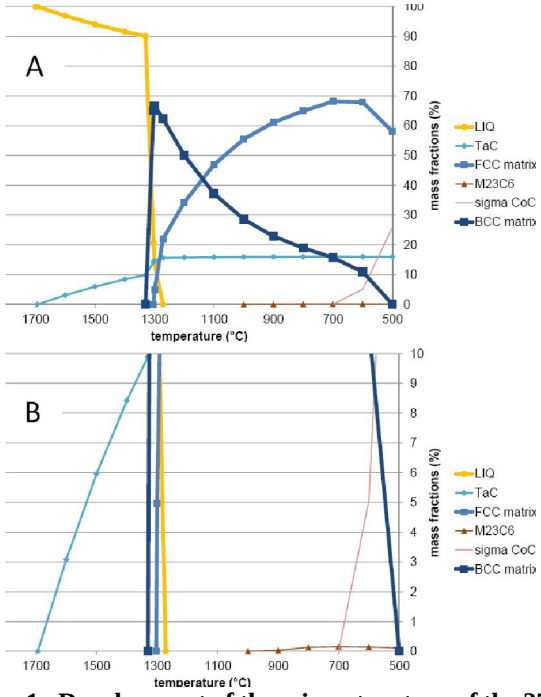

Figure 1 : Development of the microstructure of the 27Co-27Fe-30Cr-1C-15Ta alloy during solidification, according to Thermo-Calc (B: enlargement of the low mass fractions part of A)

ones are the Face Centred Cubic (FCC) TaC carbides, the chemical composition of which is {94.07Ta-5.77C-0.14Cr-0.01Co-0.01Fe (in wt.%)} at this time. Their mass fraction increases during cooling, to reach 9.89% at 1330.28°C when the second solid phase starts to appear. This second phase is BCC, and its chemical composition at its appearance, {38.21Cr-33.27Fe-26.87Co-1.64Ta-0.01C}, shows that it is the matrix. When temperature has decreased to 1303.30°C a third solid phase appears: this is a second FCC matrix phase, with as initial composition {37.39Co-33.69Fe-27.98Cr-0.88Ta-0.06C}. Solidification finishes at 1271.70°C, with the disappearance of the last drop of liquid, the ultimate chemical composition of which is {37.30Cr-30.40Co-29.07Fe-2.08Ta-1.16C}. The alloy cools then from this solidus temperature down to about 900°C, with the BCC matrix the mass fraction of which decreases from 62.39% down to 22.90%, the FCC matrix the mass fraction of which – on the contrary – increases from 22.00% up to 61.11%, and the TaC phase whose mass fraction remains constant (it varies from 15.61 to 15.96% only). At 900°C 0.03 mass.% of $M_{23}C_6$ has appeared. This second carbide phase stays at least until temperature reaches 500°C but its mass fraction stays very low (0.11% at 500°C). At 600°C a sigma phase has appeared: at this temperature its mass fraction is 5.06% and its chemical composition is {68.96Cr-26.94Co-4.10Fe-0Ta-0C}; it remains at least until 500°C, with a mass fraction having increased to 25.88%.

Evolution with temperature of the mass fraction and the chemical composition phase by phase

The thermodynamic calculations, even performed for a given temperature may allow anticipating the possible chemical segregations which may occur at high temperature, during solidification as well as during the cooling in solid state. Thermo-Calc was used to determine the exact temperature of appearance of each phase over the whole temperature range of solidification, and 100°C by 100°C for the solid state cooling. The results are given as graph in the following figures (from Figure 2 to Figure 7).

The chemical evolution of the liquid phase with temperature is described in Figure 2, in which the mass fraction is also recalled. The liquid phase exists alone for temperatures higher than 1693.94°C (liquidus tem-

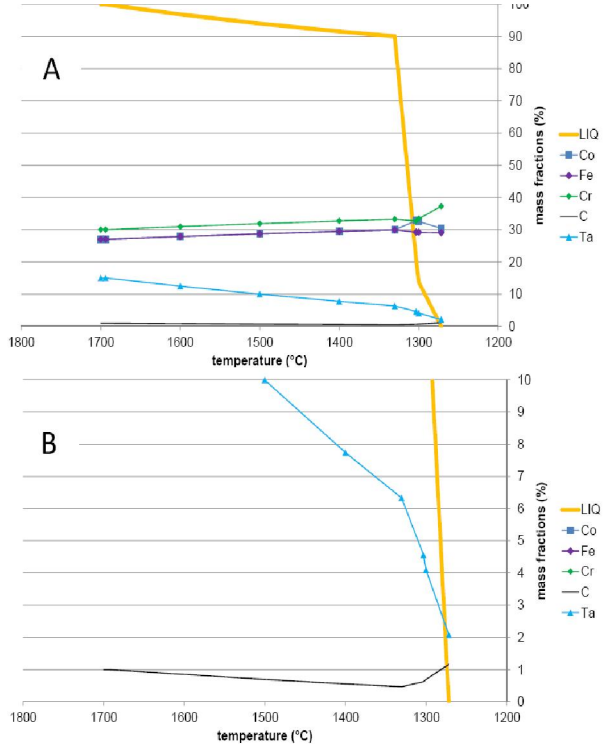

Figure 2 : Evolution of the chemical composition of the liquid phase during the cooling until its disappearance, according to Thermo-Calc (B: enlargement of the low weight contents part of A)

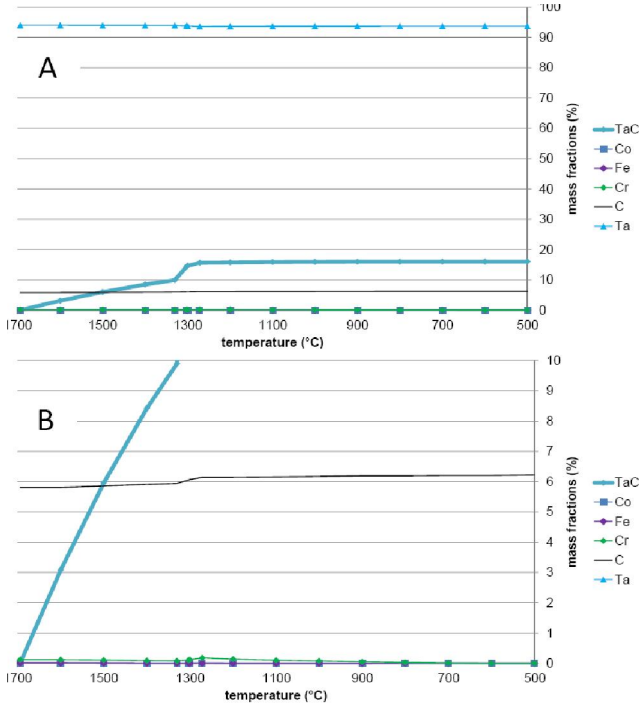

Figure 3 : Evolution of the chemical composition of the TaC phase over its temperature range of existence, according to Thermo-Calc (B: enlargement of the low weight contents part of A)

perature). Over this high temperatures range its chemical composition logically stays exactly equal to the alloy's one. When the TaC phase begins to precipitates, consuming tantalum and carbon essentially, the tantalum content and carbon content in the liquid decrease. The carbon content in the liquid suddenly increases just before the end of solidification since the carbon-poor ferritic matrix phase appears and develops, followed by the austenitic one, just a little richer in carbon. The precipitation of eutectic TaC also consumes a part of this carbon and it additionally accelerates the decrease of the tantalum content in the liquid. The latter one disappears at 1271.70°C (solidus temperature).

The first solid crystals appear at 1693.94°C. They are TaC carbides (Figure 3), which essentially contain tantalum (94.07 wt.%) and carbon (5.77 wt.%) but also traces of Cr (0.14 wt.%), cobalt (0.01 wt.%) and iron (0.01 wt.%). The greatest part of this phase develops as pro-eutectic carbides (two thirds of the total TaC) over an extended temperature interval while the rest precipitates over a much shorter temperature range, as eutectic carbides. Thereafter their mass fraction remains constant during solid state cooling down to 500°C

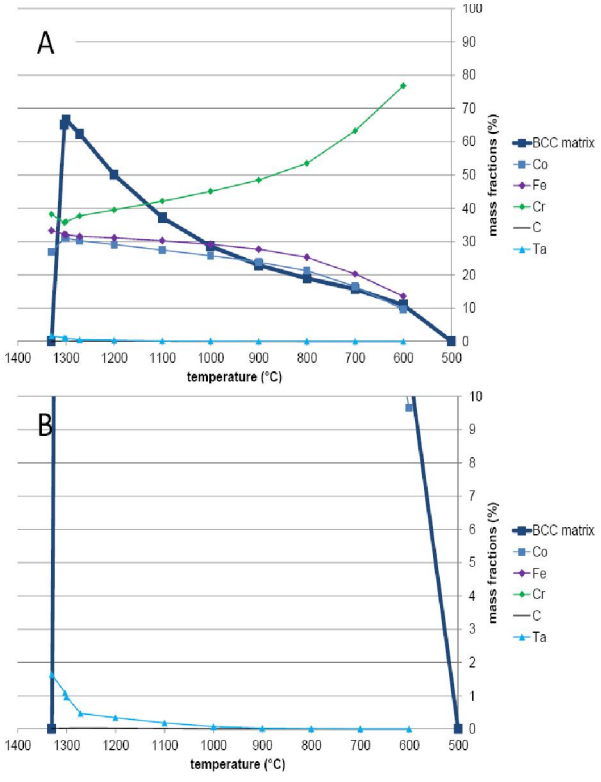

Figure 4 : Evolution of the chemical composition of the BCC matrix from its appearance to its disappearance, according to Thermo-Calc (B: enlargement of the low weight contents part of A)

(15.61% at the liquidus temperature, 15.99% at 500°C). At this same temperature the TaC phase only contains tantalum (93.78 wt.%) and carbon (6.22 wt.%) with traces of Co, Fe and Cr (less than 0.01 wt.% each).

The BCC matrix (Figure 4) appears at 1330.28°C with an initial chemical composition rich in chromium (38.21 wt.%), containing cobalt and iron in similar quantities (26.87 wt.% and 33.27 wt.% respectively) as well as tantalum in smaller quantity (1.64 wt.%), and very poor in carbon (0.01 wt.%). This is at the end of solidification that the BCC matrix is the most important since, during the subsequent cooling, its mass fraction continuously decreases to totally disappear before reaching 500°C. During its mass fraction decrease, the chromium content of this ferritic phase increases (to reach 76.80 wt.% at 600°C for example) while its iron and cobalt contents decreases (respectively 13.55 wt.% and 9.65 wt.% at 600°C). Its tantalum content decreases rapidly after the end of solidification and decreases more slowly during the subsequent cooling to reach 0.01 wt.% at 600°C. The carbon content, already very low at high temperature, as totally disappeared from this phase at 600°C at which the mass fraction of the BCC phase is only 10.91%.

In contrast with the previous ferritic matrix phase, the austenitic ones develops during the cooling (Figure 5). This second one appears shortly after the first one, 30°C under. The first crystals at 1303.30°C (temperature of FCC matrix precipitation beginning) contains {37.39Co-33.69Fe-27.98Cr-0.88Ta-0.06C, in wt.%}. The austenitic phase develops to the detriment of the ferritic one, with a mass fraction increase – first rapid but slower and slower thereafter – to reach for example 68.17% at 700°C for a phase chemical composition {35.80Co-34.94Fe-29.24Cr-0.02Ta-0.00C} not significantly modified (except Ta and C) by comparison with initially. At the same temperature it is already challenged by the sigma phase (Figure 7) which only contains chromium (68.96 wt.% at 600°C and 69.33 wt.% at 500°C), cobalt (26.94 wt.% at 600°C and 25.93 wt.% at 500°C) and iron (4.10 wt.% at 600°C and 4.74 wt.% at 500°C). The mass fraction of the FCC matrix then decreases to 58.02% for a chemical composition free of Ta and C and in which the Co and Fe contents order is inversed {44.42Fe -34.96Co-20.61Cr-0Ta-0.00C, in wt.%}.

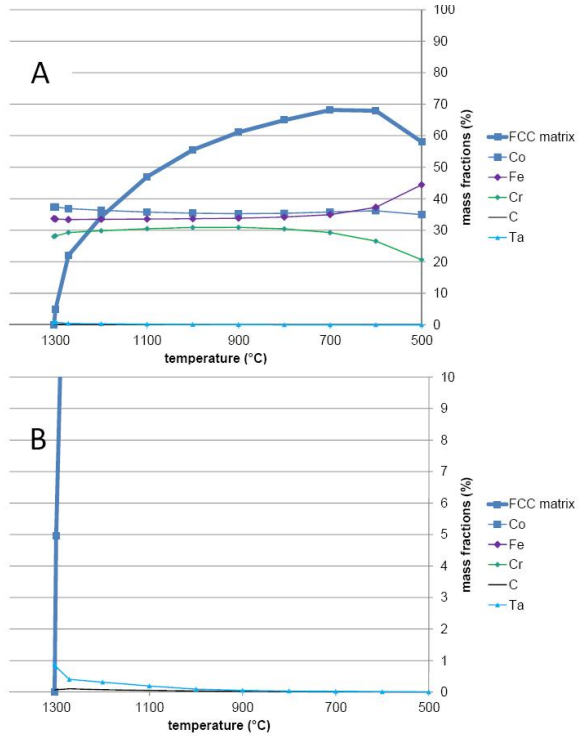

Figure 5 : Evolution of the chemical composition of the FCC matrix phase over its temperature range of existence, according to Thermo-Calc (B: enlargement of the low weight contents part of A)

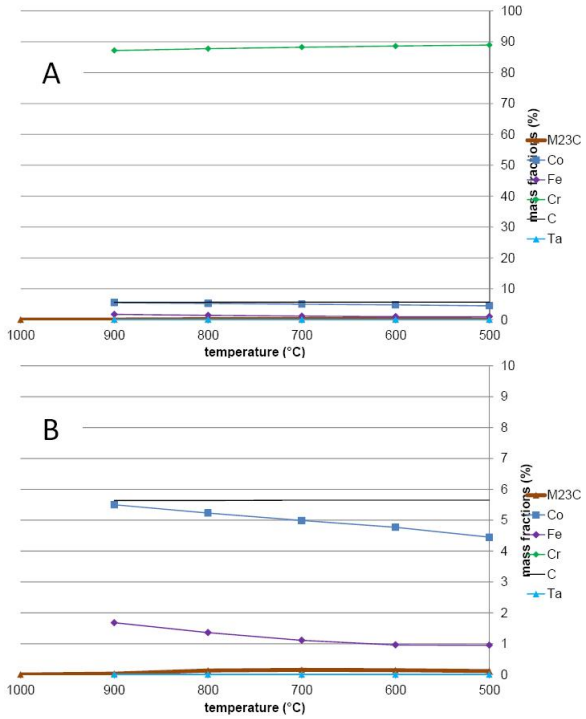

Figure 6 : Evolution of the chemical composition of the $M_{23}C_6$ phase over its temperature range of existence, according to Thermo-Calc (B: enlargement of the low weight contents part of A)

Full Paper

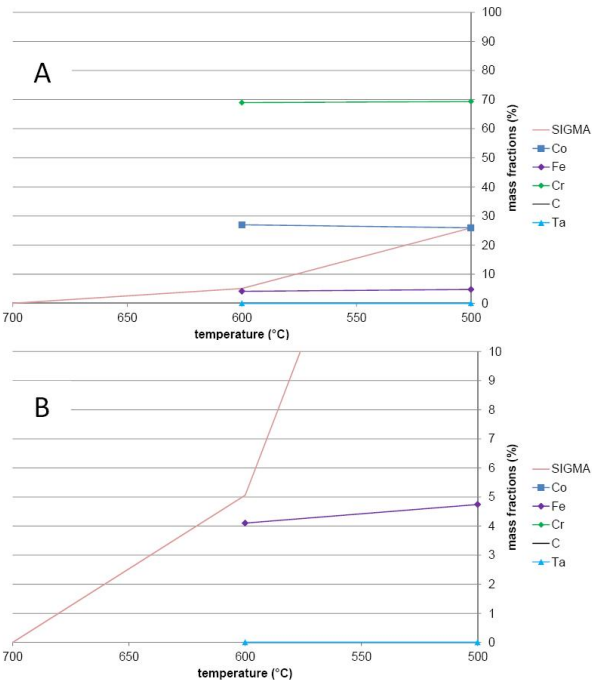

Figure 7 : Evolution of the chemical composition of the sigma phase over its temperature range of existence, according to Thermo-Calc (B: enlargement of the low weight contents part of A)

The second carbide phase, $M_{23}C_6$, appears before reaching 900°C (mass fraction 0.03% at this temperature) and stays rare at least until 500°C. Its chemical composition is very rich in chromium (87.19 wt.% at 900°C, 88.95 wt.% at 500°C) and carbon (5.64 wt.% at 900°C, 5.65 wt.% at 500°C). It also contains cobalt (5.50 wt.% at 900°C, 4.45 wt.% at 500°C) and iron (1.66 wt.% at 900°C, 0.95 wt.% at 500°C), but no tantalum whatever the temperature.

Microstructure of the {27Co – 27Fe – 30Cr - 1C – 15Ta} alloy really elaborated

After having prepared and weighed (about 40 grams for the mix) the different pure elements they were melted together under inert atmosphere. After solidification and metallographic preparation of half an ingot, the chemical composition was measured by EDS and the microstructure was examined by SEM/BSE, in several locations selected far from one another on the whole metallographic surface to reveal eventual chemical or microstructural heterogeneities.

The chemical composition appears as being rather homogeneous. It is displayed in Table 1. As we can see the targeted composition is rather respected. The microstructure of the alloy is illustrated in Figure 8 by six SEM/BSE micrographs taken in six locations chosen far from one another on the whole half ingot. EDS pinpoint measurements were carried out in the matrix, in the dark particles and in the most compact white compact particles. The obtained results (Table 2) show that the tantalum content in matrix, which elsewhere contains similar quantities of Ni, Co and Cr, is rather low (1.3 wt.%Ta). The EDS measurements also showed that the dark particles, obviously rich in chromium, are chromium carbides and the white particles, very rich in tantalum are tantalum carbides. The cumulative surface fraction of carbides, whatever their nature, is particularly important.

The surface fractions of each type of carbides were measured by image analysis. The results are presented in Table 3 for the chromium carbides and in Table 4 for the tantalum carbides. This shows more quantitatively that the carbides fractions are rather heterogeneous though the ingot, but also that the chromium carbides represent a significant surface fraction (only 7.55 ± 3.65%) but which is lower than the tantalum carbides one (11.45 ± 1.73 %). The hardness of the alloys was measured in the same locations where the micrographs of Figure 8 were taken, by Vickers indentation under a load of 30kg. The results, given in Table 5, shows that the obtained hardness (around 430) is not very high despite of the quantity of carbides.

General commentaries

The great weight contents in tantalum and carbon introduced in the studied alloy led to a rather dense precipitation of carbides during solidification. Many of them precipitated very early during solidification. The TaC phase was the first solid one to appear (as shown by the thermodynamic calculations), before the BCC matrix (dendritic as seen in the micrograph of the real

TABLE 1: The EDS-measured chemical composition of the real alloy

Weight percent	Co (targeted: 27)	Fe (targeted: 27)	Cr (targeted: 30)	Ta (targeted: 15)	C (targeted: 1)
Chemical composition of the alloy	26.41 ± 0.33	26.79 ± 0.13	30.69 ± 0.74	16.11 ± 0.93	Not measured

TABLE 2 : The EDS-measured chemical composition of the matrix

Weight percent	Co	Fe	Cr	Ta	C
Chemical composition of the alloy	33.32 ± 0.71	33.43 ± 0.42	31.95 ± 0.58	1.30 ± 0.18	Not measured

TABLE 3 : The surface fractions of the chromium carbides as measured by image analysis on the micrographs presented above in Figure 8

Localization	BGH	CM	BDH
	BGB	BCB	BDB
Values (surf.%)	3.44	13.81	8.61
	8.09	6.67	4.70
Average ± std deviation	7.55 ± 3.65		

TABLE 4 : The surface fractions of the tantalum carbides as measured by image analysis on the micrographs presented above in Figure 8

Localization	BGH	CM	BDH
	BGB	BCB	BDB
Values (surf.%)	12.33	12.42	9.05
	13.67	9.86	11.38
Average ± std deviation	11.45 ± 1.73		

alloy). A significant part of the TaC carbides, the most present type of carbides, is of the pro-eutectic nature, while the complementary TaC are eutectic ones, mixed with matrix. In contrast with the thermodynamic calculations which predicted that almost no chromium carbides will appear ($M_{23}C_6$ mass fraction 0.1% and less) as-cast microstructure displays a significant population of chromium carbides, in lower surface fractions than for TaC but in the same order of magnitude. Thermo-Calc calculations showed that the matrix, initially of the BCC type, ought to be progressively replaced by the FCC type. Since only type of matrix seems existing in the as-cast microstructure (no contrast brightness/difference all along the dendritic network, it seems that only one of the two matrix type exists in the alloy cooled to room temperature. Since the chromium content is of about 32 wt.% (Table 2) without significant dispersion, one can think that it is the FCC type which is present (the BCC one should be more reach in chromium, as seen in Figure 4). If no BCC seems existing, it metallographically appears that it is probably also the case for the sigma (Fe,Co)Cr phase. The transformation of the BCC matrix – if it really existed at high temperature - into the FCC one was total. A comparison of the Cr and Ta contents in the FCC matrix at all temperatures with the ones measured by EDS in the as-cast microstructure is done in Figure 9 for chromium and in Figure 10 for tantalum. For Cr the correspondence is the best at 1000 or 900°C while, for Ta, the correspondence is the best near 1300°C, as is to say, close to the end of solidification. One can think then that the FCC matrix was probably the single matrix type to appear (logical since FCC is the stable high temperature crystalline network for both Co and Fe but it is true that 30 wt.% of Cr are also present!) and that the tantalum content did not significantly evolve during solid state cooling, which is in accordance with the high stability of TaC at all temperatures the constant mass fraction of which was also here revealed by Thermo-Calc.

A matrix still austenitic after cooling to room temperature may explain the rather high level of hardness (average value of 430 Hv30kg) shown by the as-cast alloy. A part of this increased hardness by comparison with the NiCo-based alloy of the first part of this work[27], may be attributed to the additional presence of 7-8

TABLE 5 : The hardness values obtained in the areas where the micrographs presented above in Figure 8 were taken

Localization	BGH	CM	BDH
	BGB	BCB	BDB
Values (surf.%)	12.33	12.42	9.05
	13.67	9.86	11.38
Average ± std deviation	11.45 ± 1.73		

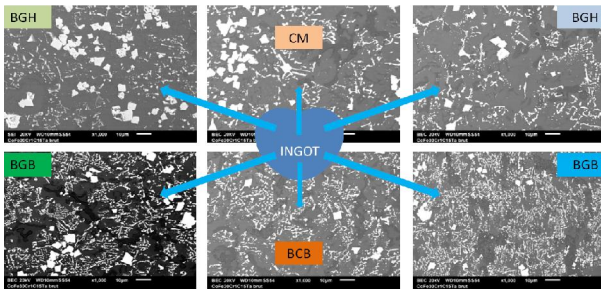

Figure 8 : The as-cast microstructures of the studied alloy in several locations of the half part of the ingot (symbolized in red)

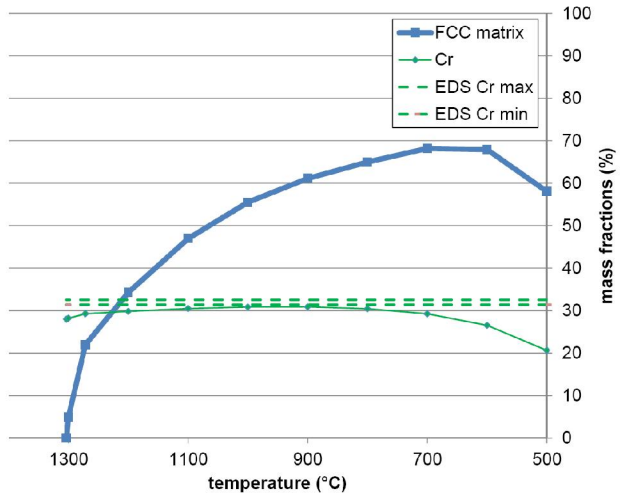

Figure 9 : Comparison of the real chromium content determined by EDS analysis in the ingot (average value ± standard deviation, two dashed horizontal green lines) with the FCC matrix chromium evolution with temperature calculated with Thermo-Calc

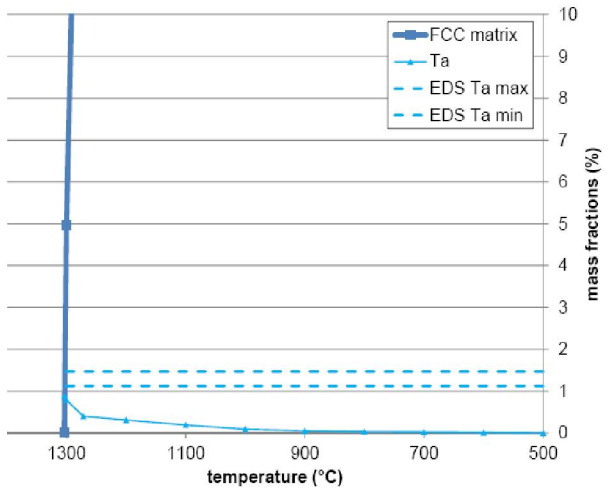

Figure 10 : Comparison of the real tantalum content determined by EDS analysis in the ingot (average value ± standard deviation, two dashed horizontal green lines) with the FCC matrix tantalum evolution with temperature calculated with Thermo-Calc stirring.

mass.% of chromium carbides here, but also to the matrix which is the hard FCC one instead the softer BCC one.

One can compare the obtained microstructure with what was observed in other previous works concerning a Co-30Cr-1C-15Ta alloy[28] and a Fe-30Cr-1C-15Ta alloy[29]. The same types of microstructures were encountered with this cobalt-based alloy and this iron-based one: dendritic matrix, blocky pro-eutectic TaC carbides in the Co-based alloy (identified thanks to Thermo-Calc too), other TaC forming a script-like eutectic with matrix, and presence of numerous chromium carbides in the Fe-based alloy. There are also differences in the microstructural point of view: the carbide fraction seems higher in the present case than for the Co-based and the Fe-based alloy. In the present CoFe-based alloy, there are many chromium carbides while the eutectic TaC carbides and the pro-eutectic TaC ones are simultaneously present in great quantities. As to supposed in the first part of this work[27], the presence of many blocky TaC carbides can be due to a limitation of the outwards migration of many of the pro-eutectic TaC carbides under the electromagnetic stirring However, the temperature range of solidification (Thermo-Calc calculations) is medium and not lower than for the two previous alloys. Indeed $T_{liquidus} - T_{solidus}$ = 1694 – 1272 = 422°C for the CoFe-based alloy which is, on the contrary higher the 150°C calculated for the Co-based one[28], which will be more favourable to a TaC migration. In contrast the solidification temperature range of the present alloy is lower than the about 600°C calculated for the Ni-based one[28]. Similarly, the temperature range of pro-eutectic TaC freedom in the melt is here higher than for the previous alloys: $T_{liquidus} - T_{solidus}$ = 1694 – 1330 = 364°C for the CoFe-based alloy is higher than the about 140°C calculated for the Co-based one[28]. But it is lower than the 450°C calculated for the Fe-based one[29]. Thus the time available for the growing pro-eutectic TaC to migrate towards the external surface of the semi-molten alloy was greater either higher or lower than for the two previous Co-based and Ni-based alloy for which much more blocky TaC migrated in the periphery of the ingot, by comparison with the present CoFe-based alloy. Thus the understanding of the dependence between the temperature range of solidification and the amount of migrated TaC carbides, which was established in the first part of this work27 is not confirmed in the present part. Nevertheless, one can say that the greater carbide fraction (TaC + chromium carbides) helped the present alloy (average 430 Hv30kg) to be close in hardness to the hard Co-based one[28] (average 440, Co-based matrix intrinsically hard) and harder than the ferritic Fe-based alloy[28] (average 266). But all these values of hardness are under the ones earlier obtained for Co-based[30] and Fe-based[31] alloys highly strengthened by chromium carbides only.

CONCLUSIONS

In this second double base CoFe too the addition of 1 wt.% of carbon and 15wt.% of tantalum led to numerous TaC carbides, of two types again: pro-eutectic and eutectic. The 30 wt.% of chromium promoted the additional formation of many chromium carbides, which was in disagreement with what the preliminary thermodynamic calculations predicted. As for the NiCo-based alloy studied in the first part of this work, many blocky pro-eutectic carbides were kept in the whole ingot, trapped by solidification. But this fact is not so easily explicable as in the first part. One can suppose that the thermo-kinetic conditions of solidification did not respect the successive thermodynamic equilibria. It is also possible that the database used for Thermo-Calc calculations is not accurate enough to allow sufficiently good predictions for the solidification temperature range, as this was also seen for the quantity of chromium carbides and the type of matrix (which remains to be verified by X-ray diffraction).

REFERENCES

[1] D.A.Bridgeport, W.A.Brandtley, P.F.Herman; Journal of Prosthodontics, **2**, 144 **(1993)**.

[2] C.T.Sims, W.C.Hagel; The superalloys, John Wiley & Sons, New York, **(1972)**.

[3] P.Berthod, J.L.Bernard, C.Liébaut; Patent WO99/16919.

[4] P.Kofstad; High Temperature Corrosion, Elsevier applied science, London, **(1988)**.

[5] E.F.Bradley; Superalloys: A Technical Guide, ASM International, Metals Park, **(1988)**.

[6] B.Roebuck, E.A.Almond; Int.Mater.Rev., **33**, 90 **(1988)**.

[7] A.Klimpel, L.A.Dobrzanski, A.Lisiecki, D.Janicki; J.Mater.Process.Tech., **164-165**, 1068 **(2005)**.

[8] K.Kishitake, H.Era, F.Otsubo; Scr.Metall.Mater., **24**, 1269 **(1990)**.

[9] A.Litwinchick, F.X.Kayser, H.H.Baker, A.Henkin; J.Mater.Sci., **11**, 1200 **(1976)**.

[10] H.E.N.Stone; J.Mater.Sci., **14**, 2787 **(1979)**.

[11] B.V.Cockeram; Metall.Trans.A, **33**, 3403 **(2002)**.

[12] E.F.Ryntz, H.L.Arnson; Modern Casting, **66**, 53 **(1976)**.

[13] Thermo-Calc version N: Foundation for Computational Thermodynamics Stockholm, Sweden, Copyright, **(1993, 2000)**.

[14] SGTE: Scientific Group Thermodata Europe database, update, http://www.SGTE.org, **(1992)**.

[15] A.Fernandez Guillermet; Int.J.Thermophys., **8**, 481 **(1987)**.

[16] J.O.Andersson; Int.J.Thermophys., **6**, 411 **(1985)**.

[17] P.Gustafson; Carbon, **24**, 169 **(1986)**.

[18] A.Fernandez Guillermet; Z.Metallkde, **78**, 700 **(1987)**.

[19] J.O.Andersson; Calphad, **11**, 271 **(1987)**.

[20] A.Fernandez Guillermet; Z.Metallkde, **79**, 317 **(1988)**.

[21] K.Frisk, A.Fernandez Guillermet; J.Alloys Compounds, **238**, 167 **(1996)**.

[22] Z.K.Liu, Y.Austin Chang; Calphad, **23**, 339 **(1999)**.

[23] N.Dupin, I.Ansara ; J.Phase Equilibria, **14**, 451 **(1993)**.

[24] P.Gustafson; Scan. J.Metall., **14**, 259 **(1985)**.

[25] J.O.Anderson, B.Sundman; Calphad, **11**, 83 **(1987)**.

[26] J.O.Anderson; Met.Trans.A, **19A**, 627 **(1988)**.

[27] L.Corona, P.Berthod; Materials Science: An Indian Journal, **10(4)**, 152 **(2014)**.

[28] L.Corona, P.Berthod; Materials Science, An Indian Journal, **10(7)**, 247 **(2014)**.

[29] P.Berthod, O.Hestin, E.Souaillat, P.Lemoine, G.Michel, L.Aranda; Annales de Chimie – Science des Matériaux, **36(3)**, 193 **(2011)**.

[30] P.Berthod, A.Dia, M.Ba, P.Lemoine, P.Villeger; Annales de Chimie – Science des Matériaux, **36(1)**, 27 **(2011)**.